Zero-current switching series loaded resonant converter insensitive to resonant component tolerance for battery charger

Junsung Park, Minjae Kim, Sewan Choi

Department of Electrical and Information Engineering, Seoul National University of Science and Technology,
172 Kongneung-Dong, Nowon-Ku, Seoul 139-743, Korea
E-mail: schoi@seoultech.ac.kr

Abstract: This study proposes an electric vehicle (EV) battery charger with a fixed frequency zero-current-switching (ZCS) series loaded resonant converter (SRC). Owing to the proposed fixed frequency operation the SRC is capable of operating under ZCS turn on and turn off regardless of voltage variation or load variation, and the magnetic components and the electromagnetic interference (EMI) filters can be optimised. The proposed battery charger has minimum component count, which makes it possible to achieve low cost and high reliability. Also, it is insensitive to resonant component tolerances and therefore suitable for high volume manufacturing. Experimental results are provided from a 3.3 kW prototype which was built for 2011 Future Energy Challenge Competition.

1 Introduction

Recent improvements in lithium-ion battery technology are making EVs and plug-in hybrid electric vehicles (PHEVs) a viable solution to reduce petroleum consumption and emissions in the transportation sector. Lithium-ion batteries will play an important role in automotive industries because of various advantages over other battery technologies such as the high specific energy and the high specific power, which are very important for EV and PHEV applications [1]. The customer expects batteries to be charged fast but reliably in order to avoid damaging the battery or reducing its lifetime. In order to accommodate these stringent requirements, today's battery chargers must be equipped with the extensive charging process with multiple control loops and a wide range of safety detection mechanisms and end-of charge criteria [2]. The EV battery charger must ensure that the utility current is drawn at unity power factor in order to minimise the line distortion and maximise the real power available from the utility outlet [3]. The battery charger should have high efficiency and high power density because of limited space and high fuel economy requirements. In response to these concerns, several battery chargers have recently been proposed for EV and PHEVs [4–13].

In general, the battery charger for EV has two power stages: an AC–DC stage for rectification and power factor correction and a DC–DC stage for isolation and output regulation. The DC–DC stage could be either PWM converters [4–8] or resonant converters [9–13], respectively. Fig. 1 shows the typical switch voltage and current waveforms of the two types of converters for the DC–DC stage. In general, as shown in Fig. 1a, the soft switching PWM DC–DC converter

could achieve zero-voltage-switching (ZVS) turn on of switches but usually has large turn-off switching losses. In contrast, as shown in Fig. 1b, the series loaded resonant converter (SRC) which is generally frequency controlled not only could achieve ZVS turn on of switches if operated above resonant but usually has smaller turn-off switching losses compared to the PWM converter. However, but the switching losses because of hard-switching turn off may be considerable under varying load and voltage condition. Further, the main drawbacks of the frequency controlled (conventional variable frequency) SRC are that it cannot be controlled at no load condition and the maximum gain is <1. The turn-off current of LLC resonant converters could be smaller than that of SRC since its magnitude is limited to the magnetising current at turn-off instant regardless of switching frequency variation. However, the large switching frequency variation makes it more difficult to optimise the magnetic components and the EMI filters [14]. Further, in general, the conventional variable frequency resonant converter has a challenging issue for high volume manufacturing associated with resonant component tolerances. The problem is more severe especially in the LLC resonant converter which has three resonant components to be adjusted.

This paper presents development of a battery charger for EV to meet the system specifications, shown in Table 1, laid down for the 2011 Future Energy Challenge Competition sponsored by IEEE PELS [15, 22]. The DC–DC stage of the proposed battery charger is a SRC with fixed duty cycle and fixed switching frequency. Instead, the boost converter in the AC–DC stage not only carries out power factor correction but also regulates battery current or battery voltage according to
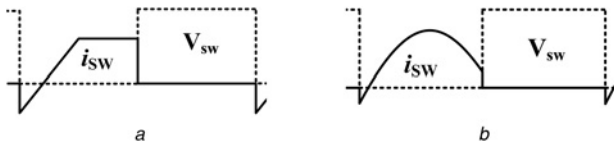
Fig. 1 *Typical switch voltage and current waveform*

a Soft switching PWM converter
b SRC

Table 1 Battery charger specification for 2011 future energy challenge competition [15]

Design item	Minimum target requirement
output power, P_o	3 kW
input voltage, V_{ac}	110 V/220 V
output voltage, V_o	332 V nominal, 250–370 V
absolute maximum voltage, V_a	410 V
power factor	higher than 0.98
efficiency	higher than 96%
communication	CAN protocol
protection	over current, over voltage, over temperature, short circuit

constant current (CC) or constant voltage (CV) commands. This makes the proposed battery charger have the following advantages over the battery charger with the conventional variable frequency SRC or LLC resonant converters.

• The proposed SRC is always capable of achieving both ZCS turn on and turn off of switches regardless of voltage and load variations.
• Owing to the fixed frequency operation the magnetic components and EMI filters of the proposed SRC can be optimised.
• The proposed battery charger is insensitive to resonant component tolerances, and therefore suitable for high volume manufacturing.
• The proposed battery charger has minimum component count, which makes it possible to achieve low cost and high reliability.

2 Proposed battery charger

The proposed battery charger consists of two power conversion stages: an AC–DC stage and an isolated DC–DC stage, as shown in Fig. 2*a*. The AC–DC stage includes a diode bridge and a boost converter. The isolated DC–DC stage is a half bridge SRC with a voltage doubler rectifier at the secondary.

The SRC in the DC–DC stage is operated at fixed frequency and fixed duty cycle and plays a simple role in galvanic isolation and adjustment of voltage gain. The boost converter in the AC–DC stage is operated to shape not only the input current for power factor correction but also directly control battery current or battery voltage for CC or CV charging operations, respectively. Therefore all the components of the isolated DC–DC stage can be designed with minimum voltage and current rating. Also, using the voltage doubler at the transformer secondary reduces the turn ratio of the transformer and helps eliminate DC magnetising offset of the transformer.

2.1 Operating principles

Figs. 2*b* and *c* show key waveforms and operation states of the proposed SRC for the illustration of the operating principle. Mode 1 begins with $L_r - C_r$ resonance when switch S_2 is turned on. Given initial values of $i_{Lr}(t_0)$ and $v_{Cr}(t_0)$, the resonant current can be determined as follows

$$i_{Lr}(t) = \left(\frac{V_o}{2n} - v_{C_r}(t_0)\right)\sqrt{\frac{C_r}{L_r}} \sin \omega_r(t - t_0) + i_{Lr}(t_0) \cos \omega_r(t - t_0) \tag{1}$$

where L_r is the resonant inductance and C_r ($= C_{r1}//C_{r2}$) is the resonant capacitance. The angular resonant frequency is

$$\omega_r = 2\pi f_r = \frac{1}{\sqrt{L_r C_r}} \tag{2}$$

Note that S_2 is turned on with ZCS, but there exists turn-on losses associated with energy stored in MOSFETs' output capacitances as follows [16, 17]

$$P_{SW,onloss} = 0.5 C_{oss} V_{SW,ON}^2 f_{s\_SRC} \tag{3}$$

where C_{oss} is the output capacitance of MOSFETs and $V_{SW,ON}$ is the turn-on voltage of the switch, as shown in Fig. 2*b*.

If $V_{SW,ON}$ is high the turn-on loss should not be neglected. Switch S_2 is turned off at t_1 and the turn-off current of S_2, which is resonant current $i_{Lr}(t_1)$, becomes equal to peak magnetising current $I_{Lm,max}$ and can be obtained by

$$i_{Lr}(t_1) = I_{Lm,max} = \frac{\pi V_o}{4n\omega_r L_m} \tag{4}$$

Since the magnetising inductance L_m of the SRC is generally made very large, $I_{Lm,max}$ is very small, resulting in negligible switch turn-off losses. During mode 2, the output capacitors of S_2 and S_3 are charged and discharged by $I_{Lm,max}$. The charging and discharging operation may not be completed because of small value of $I_{Lm,max}$, which causes a voltage $V_{SW,ON}$ across S_3 which is determined by

$$V_{SW,ON} = V_i - \frac{I_{Lm,max} D_d T_s}{2 C_{oss}} \tag{5}$$

where D_d is the duty cycle for dead time between turn off of S_2 and turn on of S_3. This voltage leads to turn-on losses regarding (3). In the proposed SRC, fortunately, $V_{SW,ON}$ can be reduced by increasing $D_d T_s$. However, increased $D_d T_s$ may cause increased current ratings and undesired resonance, and hence it should properly be chosen. In summary, the turn-off switching losses of the proposed SRC is negligible. The turn-on switching losses of the proposed SRC could be made negligible by properly choosing $D_d T_s$.

To make the discussion easier the proposed fixed frequency SRC and a conventional variable frequency SRC for the DC–DC stage of the battery charger are designed according to the design specification shown in Table 1. Fig. 3*a* shows the voltage gain curves according to load variation of the conventional variable frequency SRC. The voltage gain of the SRC can be obtained by [10] (see (6))

$$\text{Gain} = \frac{1}{1 + j(\pi^2/8R_o)\sqrt{(L_r/C_r)}\left(2\pi f_s\sqrt{L_r C_r} - (1/2\pi f_s\sqrt{L_r C_r})\right)} \tag{6}$$
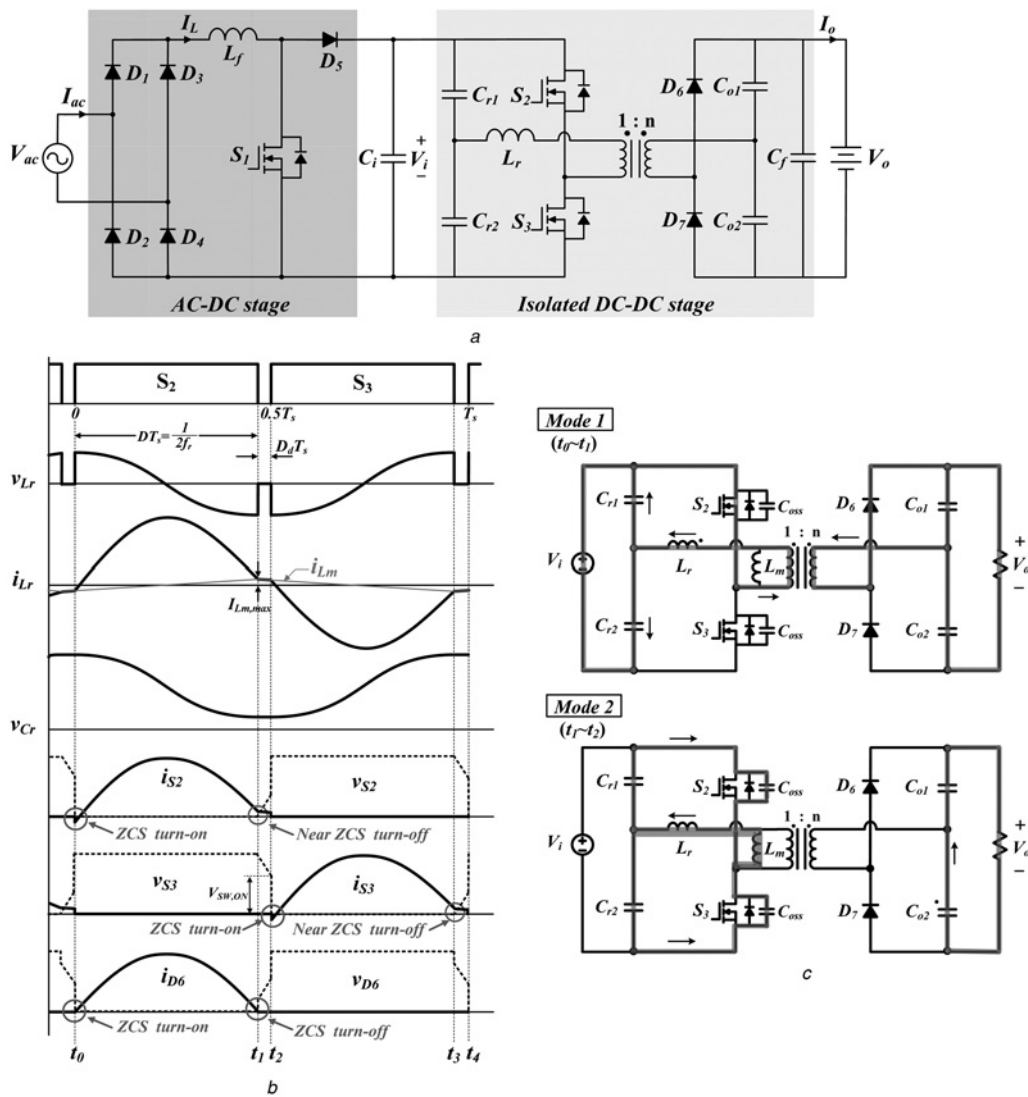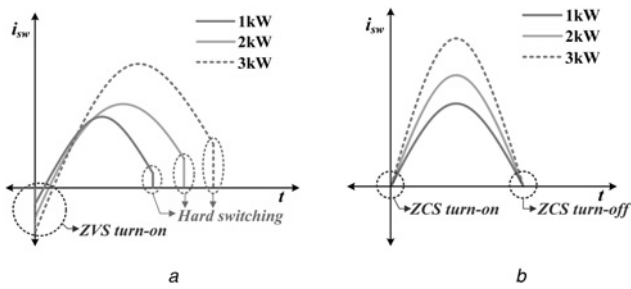
Fig. 2 *Proposed battery charger*

a Circuit diagram
b Key waveforms of the proposed SRC
c Operation states of the proposed SRC
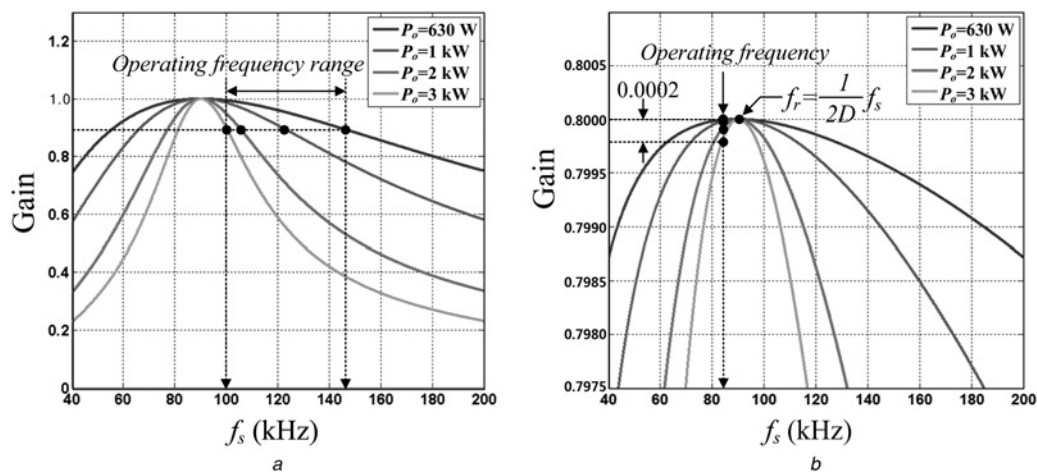
Fig. 3 *Voltage gain curve according to load variation*

a Variable frequency control
b Proposed fixed-frequency control

Fig. 4 *Switch current waveforms*

a Variable frequency control
b Proposed fixed-frequency control

The switching frequency of the conventional variable frequency SRC should vary widely to maintain the same voltage gain under load variation. It is also seen from Fig. 4*a* that as the load decreases the turn-off current decreases, but switching frequency increases. Therefore in order to reduce the switching frequency range resonant inductance should be made large in the conventional variable frequency SRC, which forces use of a separate resonant inductor. In contrast, the proposed SRC is intended to operate at fixed switching frequency, but gain variation according to load change could be made very small, as shown in Fig. 3*b*, by using the small value of L_r. This also allows the resonant inductor to be easily embedded in the transformer. Also, the proposed SRC is able to achieve ZCS turn on and turn off of the switch without regard to load variation, as shown in Fig. 4*b*, by determining the resonant frequency f_r as follows

$$f_r = \frac{1}{2D}f_{s\_SRC} = \frac{1}{1 - 2D_d}f_{s\_SRC} \qquad (7)$$

## 2.2 Effect of resonant components' tolerance

Fig. 5 shows the voltage gain and turn-off current according to resonant component tolerance. The effective resonant frequency is defined by

$$f_{r(eff)} = \frac{1}{2\pi\sqrt{L_{r(eff)}C_{r(eff)}}} \qquad (8)$$

where $L_{r(eff)}$ and $C_{r(eff)}$ are the effective resonant inductance and capacitance, respectively, reflecting component tolerances. In the conventional variable frequency SRC where L_r should be made large to reduce the switching frequency range, resonant component tolerances may cause a large shift of voltage gain curves, as shown in Fig. 5*a*, introducing additional regulation issues in particular at heavy loads [14]. That is, in order to maintain the same voltage gain, decreased $L_{r(eff)}C_{r(eff)}$ or increased $f_{r(eff)}$ causes an increase in the switching frequency, leading to increased switching losses whereas increased $L_{r(eff)}C_{r(eff)}$ or decreased $f_{r(eff)}$ causes a decrease in the switching frequency, leading to possible saturation of magnetic devices.

In contrast, in the proposed fixed frequency SRC the resonant inductance is made small to reduce the gain variation under load variation. This also leads to small voltage gain variation according to resonant component tolerances, as shown in Fig. 5*b*, which makes the proposed SRC far less sensitive to the resonant component tolerances, eliminating the voltage regulation issues and saturation
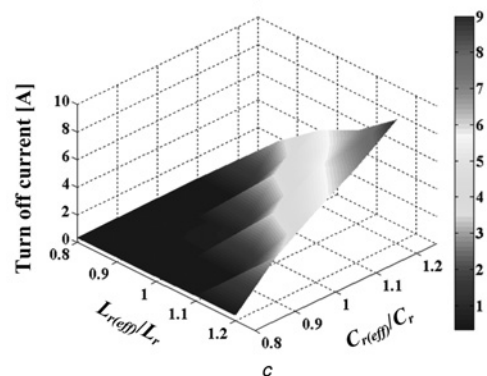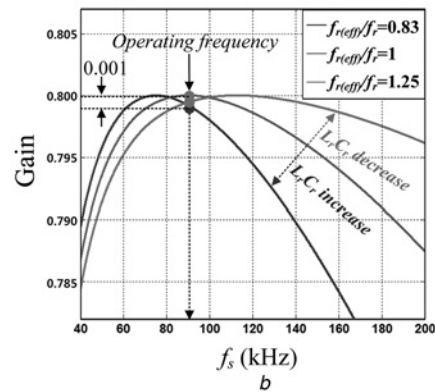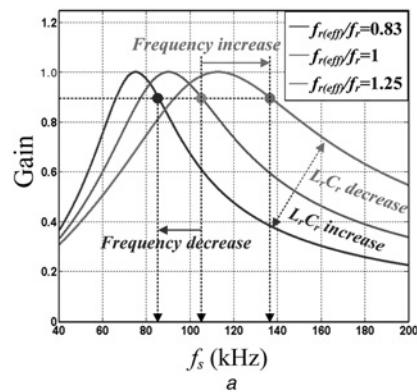
Fig. 5 *Voltage gain and turn-off current according to resonant component tolerance*

a Voltage gain of the variable frequency control ($L_r = 150\ \mu H \pm 20\%$, $C_r = 26.4\ nF \pm 20\%$)
b Voltage gain of the proposed fixed-frequency control ($L_r = 15.5\ \mu H \pm 20\%$, $C_r = 200\ nF \pm 20\%$)
c Turn-off current of the proposed fixed-frequency control ($L_r = 15.5\ \mu H \pm 20\%$, $C_r = 200\ nF \pm 20\%$)

problem of magnetic devices introduced in the conventional variable frequency SRC.

Furthermore, as shown in Fig. 5*c*, the turn-off current of the proposed fixed frequency SRC according to resonant component tolerance becomes larger as $L_{r(eff)}C_{r(eff)}$ becomes larger but is shown to have small value in most of the tolerance.

2.3 Design example

In this section, design of the boost converter and SRC components is carried out according to specification listed in Table 1. The output voltage V_o of the proposed battery charger can be expressed as

$$V_o = \frac{2\sqrt{2}nDV_{ac}}{1 - D_b} \qquad (9)$$

where n is the turn ratio of the transformer, D_b is the duty cycle of the boost converter and $D\,(=0.5-D_d)$ is the duty cycle of the proposed SRC. Therefore the range of the turn ratio can be determined as follows

$$\frac{(1-D_{b,max})V_{o,max}}{2\sqrt{2}DV_{ac,min}} < n < \frac{(1-D_{b,min})V_{o,min}}{2\sqrt{2}DV_{ac,max}} \qquad (10)$$

where the maximum duty cycle $D_{b,max}$ of the boost converter is assumed to be 0.75 and the minimum duty cycle $D_{b,min}=0$. In this example D_dT_S is chosen to be 10% of half of the switching period to reduce the turn-on losses associated with (3) and (5). That is, $D_d=0.05$ and $D=0.45$, which gives $0.66<n<0.89$. The turn ratio n is chosen to be 0.8 since the voltage rating of the switch becomes lower as the turn ratio increases. Considering the space limit of the proposed battery charger PC44PQ50/50 is chosen as a transformer core. Then the switching frequency of the proposed SRC can be obtained using the following equation [18]

$$f_{s\_SRC} > \frac{2I_{pri,rms}V_{pri,max}}{Jk_fB_mA_p} \qquad (11)$$

where $A_P=14.2$ cm^4 is the area product, $J=3$ A/mm^2 is the current density, $k_f=0.3$ is the window fill factor and $B_m=0.245$ T is the flux density. Also, the maximum primary winding voltage and the minimum primary winding current can be obtained, respectively, using the following equation

$$V_{pri,rms} = \frac{V_{o,max}}{2n} \qquad (12)$$

$$I_{pri,rms} = \frac{\pi n P_o}{\sqrt{2}V_{o,min}} \qquad (13)$$

From (11)–(13) the switching frequency of the proposed SRC is calculated as $f_{s\_SRC} > 84.8$ kHz and is chosen to be 85 kHz. Then, from (7) the resonant frequency becomes 91.7 kHz. The resonant inductance L_r and capacitances C_r can be chosen using (2). L_r should be chosen as small as possible in order to have small gain variation with regards to

component tolerances and embed it into the transformer. In this example L_r is chosen to be 15.5 µH and then C_r is 200 nF.

Boost inductance L_f can be obtained using the following equation [19]

$$L_f = \frac{D_b(1-D_b)V_o}{\Delta I_{Lf}f_{s\_boost}} \qquad (14)$$

where $\Delta I_{Lf}<15\%$ of input current, f_{s_boost} is chosen to be 35 kHz considering the volume and efficiency of the boost converter, and worst-case value of D_b is 0.5. From (14) boost inductor L_f is chosen to be 1.2 mH.

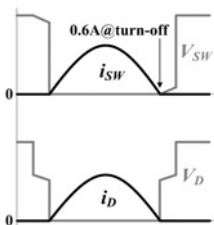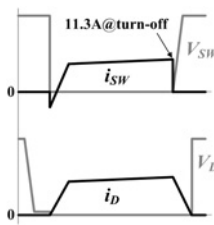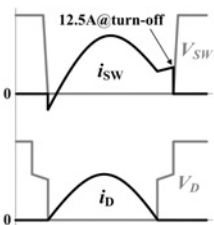Bus capacitance C_i can be obtained using the following equation [19]

$$C_i = \frac{nI_o}{2\pi f_L \Delta V_i} \qquad (15)$$

where $f_L=60$ Hz, $I_o=8.1$ A, $n=0.8$ and $\Delta V_i<5\%$ of bus voltage. From (15) bus capacitor C_i is chosen to be 1100 µF.

3 Comparative analysis

In this section, the proposed fixed frequency SRC is compared with the conventional converters including the full-bridge PWM converter in [4] and variable frequency LLC resonant converter in [9], in terms of main characteristics and device ratings. The comparison results are summarised in Table 2. All converters are turned on with ZVS or ZCS. The proposed SRC is also turned off with ZCS whereas the full-bridge PWM converter and LLC resonant converter have large turn-off currents, respectively. The LLC resonant converter has the largest transformer kVA rating because of the considerable magnetising current. The proposed SRC will have zero magnetising DC-offset of the transformer because of connection of resonant capacitor at the primary and voltage doubler at the secondary. The operation of the variable frequency LLC resonant converter is sensitive to resonant component tolerances, which causes possible saturation of magnetic devices. The proposed SRC has the lowest component count, which makes it possible to achieve low cost and high reliability.

Table 2 Comparison of characteristic of the proposed and conventional converters ($P_0=3$ kW, $V_i=220$ V, $V_0=370$ V)

	Proposed SRC	Full-bridge PWM converter [4]	LLC resonant converter [9]
Control method	Fixed frequency	Duty cycle control	Variable frequency
Switch and diode waveforms			
Switch ratings			
	462V, 10A$_{rms}$	400V, 6.7A$_{rms}$	400V, 13$_{rms}$
Diode ratings	370V, 8A$_{avg}$	370V, 4A$_{avg}$	370V, 4A$_{avg}$
Transformer kVA rating	3.4 kVA	3.6 kVA	4.2 kVA
Transformer magnetising dc offset	Zero	Possible	Possible
Sensitivity to component tolerance	Good	Fair	Poor
Number of switching devices	2 switches 2 diodes	4 switches 4 diodes	2 switches 4 diodes

4 Experimental result

A 3 kW laboratory prototype of the proposed battery charger has been built under the following system parameters used in Section 2.3.

- $V_i = 313$–493 V, $f_{s\_boost} = 35$ kHz, $f_{s\_SRC} = 85$ kHz.
- $L_f = 1.2$ mH, $C_i = 1100$ μF, $L_r = 15.5$ μH.
- C_{r1}, $C_{r2} = 100$ nF, C_{o1}, $C_{o2} = 30$ μH, $N_P{:}N_S = 10{:}8$.

The system control is implemented digitally on a Texas Instruments TMS320F28335 microcontroller for flexibility and rapid implementation. The control block diagram for the proposed battery charger is shown in Fig. 6. The dual loop consists of an outer loop for CC or CV charging and an inner loop for input current wave shaping. A feed-forward (FFD) control is added to increase the inner loop gain at 120 Hz [20, 21]. The control structure of the proposed battery charger is simple in that a voltage sensor for V_i is not necessary for control, and the total number of controllers is decreased by one compared to the conventional variable frequency-based battery chargers. The proposed battery charger is operated according to an example CC–CV charging profile shown in Fig. 7. Fig. 8 shows the input voltage and current waveforms at rated power illustrating that the power factor correction circuit is properly working. The measured power factor is 0.997. The total harmonic distortion of the input current is 4.9%. Figs. 9a–c show the switch voltage and current waveforms
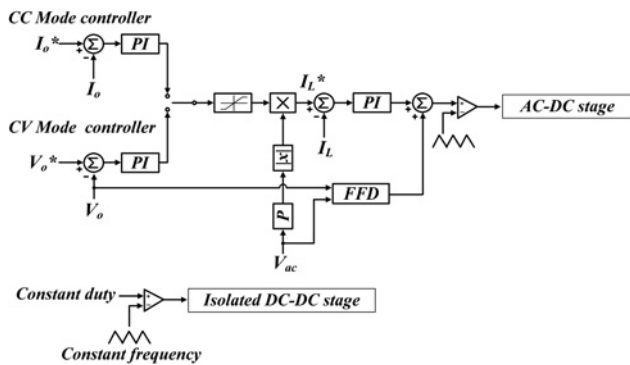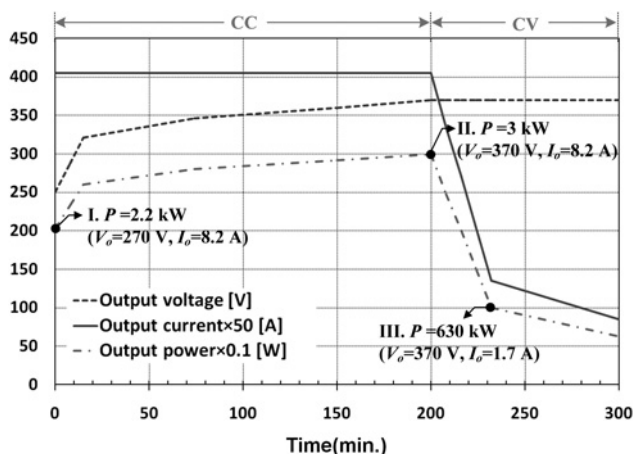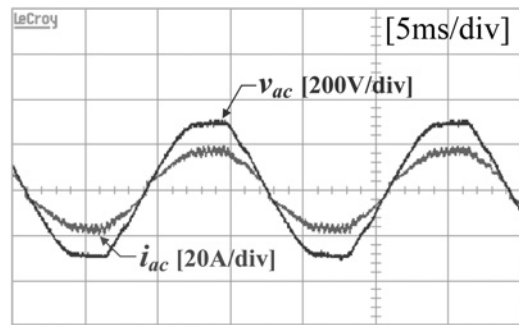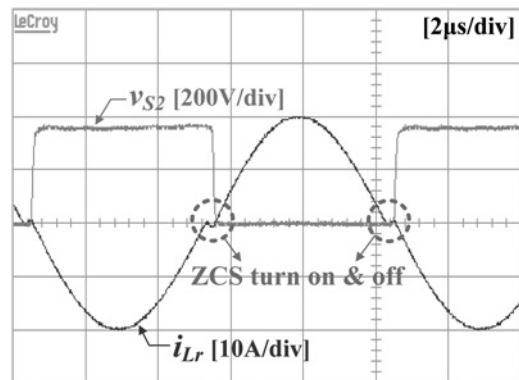

Fig. 8 *Experimental waveforms showing the input voltage and current of the proposed battery charger*

Fig. 6 *Control block diagram for the proposed SRC-based battery charger*
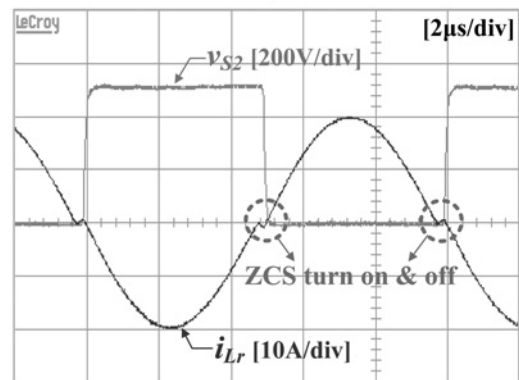

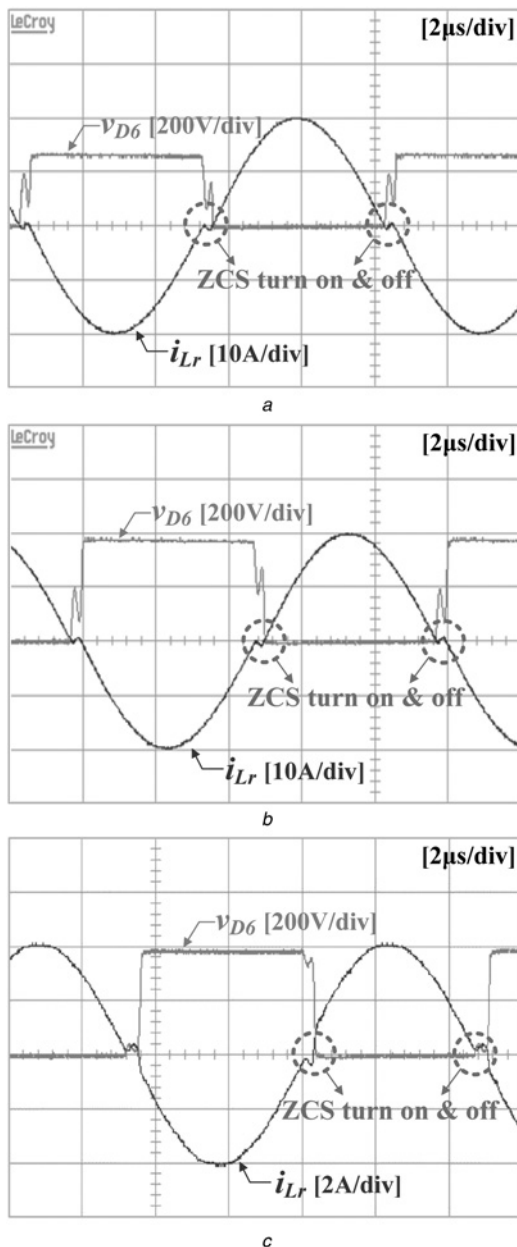**Fig. 7** *An example CC–CV charging profile*
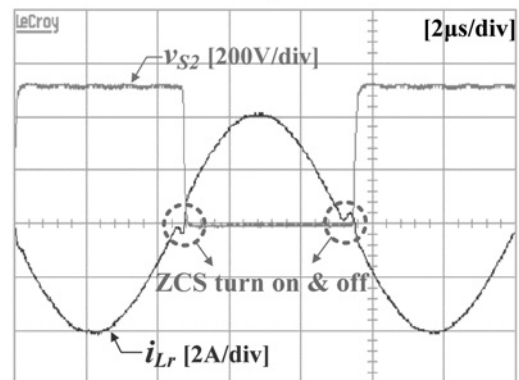
Fig. 9 *Experimental waveforms showing the switch voltage and current waveforms of the proposed battery charger*

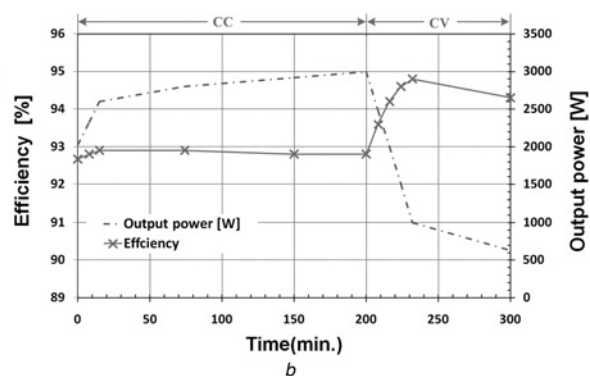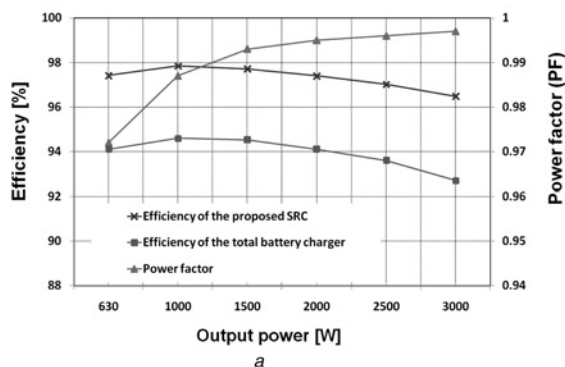*a* Operating point I of Fig. 7
b Operating point II of Fig. 7
c Operating point III of Fig. 7

Fig. 10 *Experimental waveforms showing diode voltage and current waveforms of the proposed battery charger*

a Operating point I of Fig. 7
b Operating point II of Fig. 7
c Operating point III of Fig. 7

Fig. 12 *Photograph of the proposed battery charger*

of the proposed SRC at three operating points in the example CC–CV charging profile of Fig. 7. It is seen that the switch is turned on and off with ZCS at all operating points. Figs. 10*a*–*c* show the diode voltage and current waveforms in the proposed SRC at three operating points of the example CC–CV charging profile. It is also seen that the diode is turned off with ZCS at all operating points.

Fig. 11*a* shows the measured efficiencies and power factor as a function of output power. The peak measured efficiency of the proposed SRC is 97.85% at 1 kW and full load efficiency is 96.48%. The peak measured efficiency of the total battery charger is 94.6% at 1 kW and full load efficiency is 92.7%. The peak measured power factor is 0.997 at 3 kW. Fig. 11*b* shows the measured efficiency of the proposed battery charger according to the example CC–CV charging profile. During the CC mode the efficiency of around 93% was measured. During the CV mode the efficiency was increased and the peak measured efficiency is 94.6%. All the efficiencies were measured using power analyser YOKOGAWA WT3000. Fig. 12 shows the hardware prototype of the proposed battery charger. The total volume and weight of this prototype are 7.6 L and 7 kg, respectively.

5 Conclusions

In this paper, a fixed frequency SRC-based battery charger for EV is proposed. The boost converter not only performs the power factor correction but also regulates the battery

Fig. 11 *Experimental performances of the proposed battery charger*

a Measured efficiencies and power factor as a function of output power
b Measured efficiency according to the example CC–CV charging profile

voltage and current. The proposed battery charger has the following features:

- The proposed SRC is operated under ZCS turn on and turn off regardless of voltage or load variation because of fixed frequency operation, and therefore the proposed battery charger has low switching losses and EMI.
- The proposed SRC is insensitive to resonant component tolerances since a small value of L_r can be used.
- The proposed battery charger has minimised component count and component ratings.
- The transformer of the proposed SRC shows lowest kVA rating and zero magnetising DC offset because of connection of resonant capacitor at the primary and voltage doubler at secondary.

The peak efficiency that was measured from 3.3 kW laboratory prototype is 94.6% at 1 kW and full load efficiency is 92.7%. The proposed converter could be a possible option for low-cost and high-performance battery charger for EV.

6 References

1 Marano, V., Onori, S., Guezennec, Y., Rizzoni, G., Madella, N.: 'Lithium-ion batteries life estimation for plug-in hybrid electric vehicles'. IEEE Vehicle Power and Propulsion Conf. (VPPC), Dearborn, USA, September 2009, pp. 7–10
2 Egan, M.G., O'Sullivan, D.L., Willers, M., Hayes, J.G., Willers, M.J., Henze, C.P.: 'Power-factor-corrected single-stage inductive charger for electric vehicle batteries', *IEEE Trans. Ind. Electron.*, 2007, **54**, (2), pp. 1217–1226
3 Poon, F.N.K., Pong, M.H.: 'A constant power battery charger circuit with inherent soft switching and PFC'. IEEE Applied Power Electronics Conf. (APEC), New Orleans, USA, February 2000, pp. Fi80–484
4 Gautam, D., Musavi, F., Edington, M., Eberle, W., Dunford, W.G.: 'An automotive onboard 3.3-kW battery charger for PHEV application', *IEEE Trans. Veh. Technol.*, 2012, **61**, (8), pp. 3466–3474
5 Hsieh, Y.-C., Huang, C.-S.: 'Li-ion battery charger based on digitally controlled phase-shifted full-bridge converter', *IET Power Electron.*, 2011, **4**, (2), pp. 242–247
6 Kim, T., Lee, S., Choi, W.: 'Design and control of the phase shift full bridge converter for the on-board battery charger of electric forklifts', *J. Power Electron.*, 2012, **12**, pp. 113–119
7 Whitaker, B., Barkley, A., Cole, Z., et al.: 'A high-density, high-efficiency, isolated on-board vehicle battery charger utilizing silicon carbide power devices', *IEEE Trans. Power Electron.*, 2014, **29**, (5), pp. 2606–2617
8 Gu, B., Lai, J.-S., Kees, N., Zheng, C.: 'Hybrid-switching full-bridge DC–DC converter with minimal voltage stress of bridge rectifier, reduced circulating losses, and filter requirement for electric vehicle battery chargers', *IEEE Trans. Power Electron.*, 2013, **28**, (3), pp. 1132–1144
9 Dow, Y.S., Son, H.I., Lee, H.D.: 'A study on half bridge LLC resonant converter for battery charger on board'. IEEE ECCE, Jeju, Republic of Korea, June 2011, pp. 2694–2698
10 Kim, J., Choe, G., Jung, H., Lee, B., Cho, Y., Han, K.: 'Design and implementation of a high-efficiency on-board battery charger for electric vehicles with frequency control strategy'. IEEE Vehicle Power and Propulsion Conf. (VPPC), Lille, France, September 2010, pp. 1–6
11 Chae, H.J., Moon, H.T., Lee, J.Y.: 'On-board battery charger for PHEV without high-voltage electrolytic capacitor', *Electron. Lett.*, 2010, **46**, (25), pp. 1691–1692
12 Musavi, F., Craciun, M., Gautam, D.S., Eberle, W., Dunford, W.G.: 'An LLC resonant DC–DC converter for wide output voltage range battery charging applications', *IEEE Trans. Power Electron.*, 2013, **28**, (12), pp. 5437–5445
13 Bai, H., Taylor, A., Guo, W., et al.: 'Design of an 11 kW power factor correction and 10 kW ZVS DC/DC converter for a high-efficiency battery charger in electric vehicles', *IET Power Electron.*, 2012, **5**, (9), pp. 1714–1722
14 Youssef, M.Z., Jain, P.K.: 'A review and performance evaluation of control techniques in resonant converters'. IEEE Industrial Electronics Conf. (IECON), Busan, Republic of Korea, November 2004, pp. 215–221
15 'Future Energy Challenge Competition Web Site', http://www.energychallenge.org, accessed October 2013
16 Brambilla, A., Dallago, E., Nora, P., Sassone, G.: 'Study and implementation of a low conduction loss zero-current resonant switch', *IEEE Trans. Power Electron.*, 1994, **41**, (2), pp. 241–250
17 Liu, K., Lee, F.C.Y.: 'Zero-voltage switching technique in DC/DC converters', *IEEE Trans. Power Electron.*, 1990, **5**, (3), pp. 293–304
18 Ekekwe, N., Ndubah, J.E., White, K., Ben, O.: 'Practical process in high frequency distribution transformer design'. IEEE Electrical Insulation Conf. and Electrical Manufacturing and Coil Winding Technology Conf. (EICEMC), September 2003, pp. 121–128
19 'Boost type CCM PFC design with ICE1PCS01/02', http://www.infineon.com, accessed January 2014
20 Shin, J., Hyeon, B., Cho, B.: 'Digital control of a power factor correction boost rectifier using diode current sensing technique', *J. Power Electron.*, 2009, **9**, pp. 903–910
21 Genc, N., Iskender, I.: 'DSP-based current sharing of average current controlled two-cell interleaved boost power factor correction converter', *IET Power Electron.*, 2011, **4**, (9), pp. 1015–1022
22 Park, J., Kim, M., Choi, S.: 'Fixed frequency series loaded resonant converter based battery charger which is insensitive to resonant component tolerance'. IEEE Int. Power Electronics and Motion Control Conf. (IPEMC), Harbin, China, June 2012, pp. 918–922